Residual order within the molten Al(110) surface layer

L. Pedemonte* and G. Bracco
Istituto Nazionale di Fisica della Materia and C.F.S.B.T.-CNR, Dipartimento di Fisica dell'Università di Genova, Genova, Italy

A. Robin and W. Heiland
Universität Osnabrück, FB Physik, Osnabrück, Germany
(Received 21 December 2001; published 28 May 2002)

The evolution of thermal disorder on the (110) surface of aluminum is investigated along the $\langle 1\bar{1}0\rangle$ and $\langle 001\rangle$ azimuthal directions in the temperature range between 300 and 910 K by low-energy ion scattering. Surface blocking and channeling mode and neutral impact collision ion scattering spectroscopy are used. Information is gained about the proliferation of point defects and surface roughness below the surface melting point. Surface premelting is observed using a new technique, i.e., investigating the evolution of the channeling peak with temperature. Experimental evidence for residual short-range order is obtained along both azimuths within the quasiliquid layer which probably consists of groups of surface atoms in correlated motion.

DOI: 10.1103/PhysRevB.65.245406 PACS number(s): 68.35.Rh, 68.35.Ja, 68.49.−h

I. INTRODUCTION

A great amount of experimental and theoretical studies has shown in the last years that the (110) surface of metals with fcc structure exhibits a remarkable behavior as a function of temperature because of its open atomic arrangement. Among them, Al(110) is proved to go through all the familiar stages of disorder as the crystal temperature is raised up to the bulk melting point ($T_m = 933$ K). In particular, slightly above room temperature low-energy electron diffraction (LEED) measurements point out an increased anharmonicity of the vibration amplitude of the top layer atoms and indicate it as precursor to surface preroughening observed at ~ 420 K.[1,2] With further increasing the temperature three-dimensional disorder is detected, leading the surface to roughen at 600 K.[3] At about the same temperature LEED and x-ray scattering data show a dramatic enhancement of anharmonic contributions to surface lattice vibrations.[1,4,5] Because of their large vibration amplitude, some atoms of the top layers are observed in molecular dynamic (MD) simulations to overcome the potential barrier, giving rise to surface point defects, i.e., vacancies and adatoms. Moreover, proliferation of point defects with temperature is suggested by MD as the disordering mechanism preliminary to the premelting transition.[6,7] A molten surface layer with quasiliquid properties and whose thickness rapidly increases towards the bulk melting point has been firstly detected on Al(110) above 815 K with medium-energy ion scattering (MEIS).[8] Thereafter, the most sophisticated surface-sensitive techniques have been employed to investigate premelting of this surface and its critical temperature has been measured with small indetermination. Depending on the technique, it is estimated to lie in the range between 770 and 815 K.[1,4,9–11] These studies provide a quite satisfactory picture of the evolution of thermal disorder up to surface premelting, but only little information is given about the details of the microscopic melting mechanism and about the structure of the quasiliquid layer. In particular, surface-extended x-ray-adsorption fine-structure (SEXAFS) measurements suggest that the molten layer retains anisotropic residual order which consists of intact $\langle 1\bar{1}0\rangle$ rows or segments of them with liquidlike mobility.[10,11] Recent predictions of MD calculations further support this result.[12] In order to contribute to the discussed topics, we present an investigation of the thermal behavior of the (110) surface of aluminum in the temperature range between 300 and 910 K performed by low-energy ion scattering (LEIS) using surface blocking and channeling mode and neutral impact collision ion scattering spectroscopy (NICISS). It is worth noting that LEIS is a surface-sensitive direct imaging technique which is especially suited to investigate changes in the nearest neighborhood and the development of point defects within the surface top layer. This is the reason why this technique has been successfully applied in the past to study premelting of Pb(110).[13,14]

The paper is organized as follows: Section II describes the experimental details while the results are presented and analyzed in Sec. III. In Sec. IV conclusions are finally singled out.

II. EXPERIMENT

The experiment is performed with the UHV scattering machine described in detail elsewhere.[15,16] Briefly, a 1.5-keV He^+ primary beam is produced within a plasma ion source, mass selected with a magnetic filter and pulsed sweeping it over a small aperture in front of the magnet. The scattered particles, i.e., ions and neutrals, are collected by two time-of-flight detection systems corresponding to different geometries. In detail, the scattering angle is fixed at $\Theta = 165°$ and at $\Theta = 6°$ in the backscattering and forward scattering geometries, respectively. At incident energies above 1 keV the channel plates employed for particle counting have a detection efficiency close to 1. The Al sample is mounted on a three-axis manipulator and heated radiatively. The temperature is measured using a thermocouple and a pyrometer with an uncertainty of approximately ± 15 K. The operating pressure in the main chamber is in the 10^{-10} mbar range. Since the Al surface was initially contaminated by strongly bonded oxygen atoms, we have performed repeated *in situ* cleaning cycles consisting in prolonged 4-keV, Ne^+ ion sputtering at

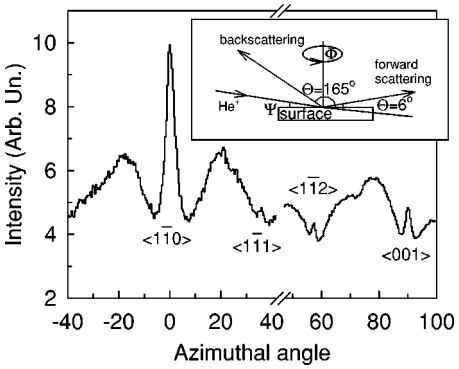

FIG. 1. Surface channeling pattern, intensity vs the azimuth angle ϕ, for He^+ at 1.5 keV, scattered from Al(110) at room temperature. The incidence angle with respect to the surface plane is $\psi=3°$; the scattering angle is $\Theta=6°$. The scattering geometry used for surface blocking, surface channeling, and NICISS experiments is sketched in the inset.

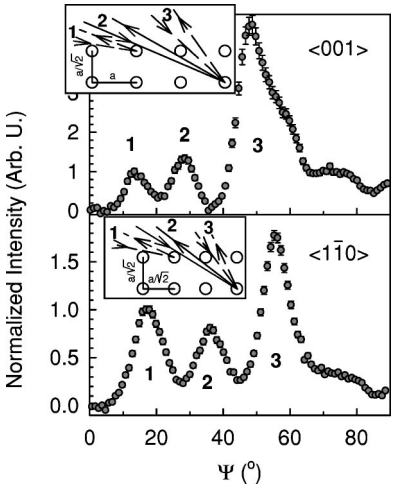

FIG. 2. Gray circles are the NICISS scans, intensity vs the incidence angle ψ, for He^+ at 1.5 keV scattered from Al(110) at $\Theta=165°$. The surface temperature is $T=310$ K. The upper and lower panels refer to the $\langle 001\rangle$ and $\langle 1\bar{1}0\rangle$ azimuthal directions, respectively. The scans are normalized to the maximum of the first focusing peak after subtraction of a constant background. In the inset a lateral view of the surface is reported showing the first and third atom layers. Here $a=4.05$ Å is the aluminum lattice constant. The trajectories which mainly contribute to the observed peaks are sketched.

crystal temperature of 420 K and at grazing incidence angle of $\sim 15°$ followed by damage annealing above 800 K. At the end of each cycle the surface chemical composition has been controlled by low-energy ion scattering spectroscopy (ISS) using an electrostatic energy analyzer mounted at scattering angle $\Theta\sim 85°$.[17] After ~ 20 cycles no oxygen is observed on the surface within the sensitivity of our ISS system for more than 5 h after cleaning. The surface structure is probed by two ion scattering modes: surface channeling and blocking. In both cases the incoming beam hits the target at a fixed grazing incidence angle ψ; thereafter, forward and backscattered particles are detected, respectively. If the azimuthal angle ϕ is rotated, the intensity I vs ϕ pattern provides a picture in real space of the surface structure showing sharp features due to surface channeling along the main crystallographic directions.[18] Maxima are observed in the forward scattering mode and deep minima in backscattering mode. The sharpness of the structures reflects the quality of the surface since defects block the surface channels and cause the spectra to flatten.[13] The azimuthal profile measured in forward scattering for a well-prepared surface is shown in Fig. 1. From the angular position of the peaks the main azimuthal directions can be set into the scattering plane within $\pm 1°$. Hence the usual NICISS data (i.e., I vs ψ scans in backscattering mode) are taken. The scattering geometry of the experiment is sketched in the inset of Fig. 1.

III. RESULTS

Typical NICISS spectra measured slightly above room temperature along the $\langle 001\rangle$ and $\langle 1\bar{1}0\rangle$ azimuthal directions are reported in Fig. 2. The first intensity maximum arises from scattering off the atomic chains (trajectory 1 in the inset) while geometrical considerations suggest that the features at large angles can be mainly ascribed to scattering contributions from the third layer (paths 2 and 3 in the inset). In order to obtain information about the structure of the top layer the first focusing peak is fitted along the two azimuths within a two-atom scattering model.[19] Here, the scattered intensity is calculated versus the incidence angle solving the scattering problem in two dimensions and using the first neighbor of the leading atom within the scattering plane as detector for the shadow cone cast by the leading one. Since in the experiment both scattered neutrals and ions are detected, the calculated intensities are comparable with the data without further adjustment. Parameters entering into the calculation are the lattice constant and the He-Al interaction potential. In particular, the intensity distribution was calculated using both the standard Ziegler-Biersack-Littmark (ZBL) potential and the Thomas-Fermi-Molière (TFM) potential with different screening lengths.[17] The best agreement with the angular position of the measured peaks is obtained with the ZBL potential giving an offset of less than 1° along both directions. Surface vacancies are included in the scattering model. In particular, if the first neighbor of the leading atom is missing, the shadow cone is cast onto the second neighbor and the corresponding scattering contribution is accounted for as a doubling of the lattice parameter.[13] Surface thermal vibrations are described as static disorder with the atoms randomly displaced from their equilibrium sites according to a two-dimensional Gaussian distribution. The ratio between the mean-square vibration amplitude perpendicular and parallel to the surface is given as input parameter. The perpendicular mean-square vibration amplitude and the vacancy percentage within the scattering plane are obtained as fitting parameters. The curves which best fit the data are reported together with the different scattering contributions in Fig. 3. It should be noted that a relevant amount of point defects is present within the top layer already at room temperature. In fact, a vacancy percentage of $(10\pm 4)\%$ and of $(8\pm 4)\%$ is estimated along the $\langle 1\bar{1}0\rangle$ and $\langle 001\rangle$ azimuths, respectively. Insight into the proliferation of surface defects

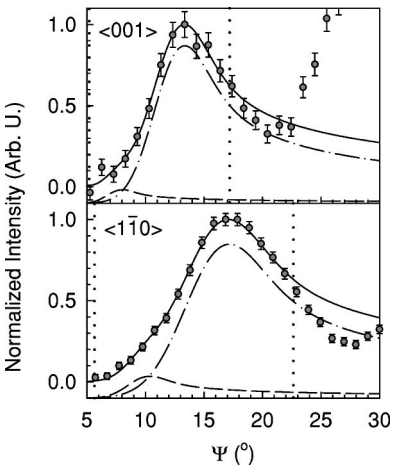

FIG. 3. The first focusing peak in the NICISS scan of Fig. 2 along the $\langle 001 \rangle$ and $\langle 1\bar{1}0 \rangle$ azimuth is compared with the corresponding best-fitting curve calculated within the two-atom model described in the text. The total scattered intensity (solid line) is obtained as the sum of contributions from the perfect surface and from surface vacancies. They are shown (with an offset of 0.1 along the *y* axis) as the dash-dotted line and dashed line, respectively. The dotted vertical lines indicate the limits of the fitted range.

with increasing temperature is provided in Fig. 4 where the NICISS scan measured at 650 K along the $\langle 1\bar{1}0 \rangle$ azimuth is reported together with the corresponding best-fitting curves. Note that scattering contributions at low incidence angle are enhanced. This is mainly due to surface defects and to the increased mean-square vibration amplitude of the top layer atoms. In particular, the measured vacancy percentage attains at 650 K the value $(24 \pm 4)\%$. Complementary information is provided in Fig. 5 where blocking patterns measured in the angular range $\phi = \pm 22°$ around the $\langle 1\bar{1}0 \rangle$ azimuthal direction and in the temperature range up to 740 K are reported. As discussed in Sec. II, at 312 K the spectra show a minimum along the $\langle 1\bar{1}0 \rangle$ azimuth which is ''filled up'' with increasing temperature because of enhanced in-plane lattice

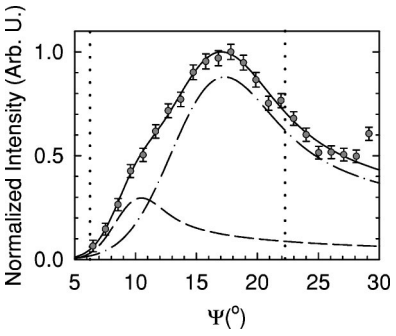

FIG. 4. Gray circles are the NICISS scan measured at surface temperature $T = 650$ K along the $\langle 1\bar{1}0 \rangle$ azimuthal direction. Data are normalized after subtraction of a constant background. Lines are the corresponding best-fitting curve. The total scattered intensity (solid line) is obtained as the sum of contributions from the perfect surface (dash-dotted line) and from surface vacancies (dashed line). Fit limits are indicated by the dotted vertical lines.

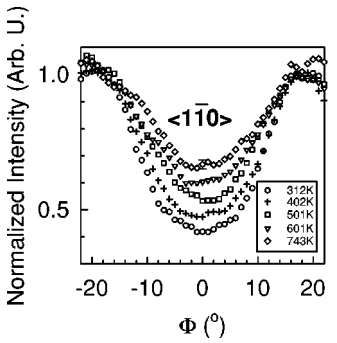

FIG. 5. Surface blocking pattern, intensity vs the azimuth angle ϕ, for He^+ at 1.5 keV scattered from Al(110) at different temperatures. The reported spectra are normalized to the intensity scattered along a high-index azimuthal direction ($\phi \sim -18.5°$). The incidence angle with respect to the surface plane is $\psi = 5°$; the scattering angle is $\Theta = 165°$.

vibrations, adatoms, and steps blocking the surface channels. In particular, comparing the measured minimum yield with those obtained at roughening on Pb(110) (Ref. 14) or Ag(110) (Ref. 20) suggestions for the onset of the roughening transition at about 600 K are obtained for Al(110). Surface roughness is less evident in Fig. 6 where the evolution with temperature of the $\langle 1\bar{1}0 \rangle$ channeling peak shape is reported. Here, at 600 K only a weak increase of the peak tail intensity can be noted. On the contrary, strong evidence is obtained for surface premelting above 800 K where the channeling peak starts to merge into the background. We remark, however, that also at the highest temperature we measured, i.e., 890 K, the channeling pattern is not completely flat, thus suggesting residual order along the $\langle 1\bar{1}0 \rangle$ azimuth within the quasiliquid layer. To complete this result, the evolution of surface disorder along the $\langle 001 \rangle$ azimuth is investigated and the NICISS profile is measured on increasing temperature up to 910 K. The result is shown in Fig. 7. Here, at low angles of incidence a strong increase of the scattered intensity accompanied by background enhancement is observed above the onset of surface premelting at ~ 800 K. However, in good agreement with the result obtained along the $\langle 1\bar{1}0 \rangle$

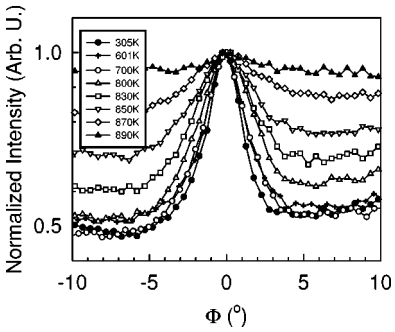

FIG. 6. Symbols show the evolution of the $\langle 1\bar{1}0 \rangle$ surface channeling peak in the temperature range between 305 and 890 K. Lines are guides for the eyes. The reported spectra are normalized at the maximum peak height. The scattering conditions are the same as in Fig. 1.

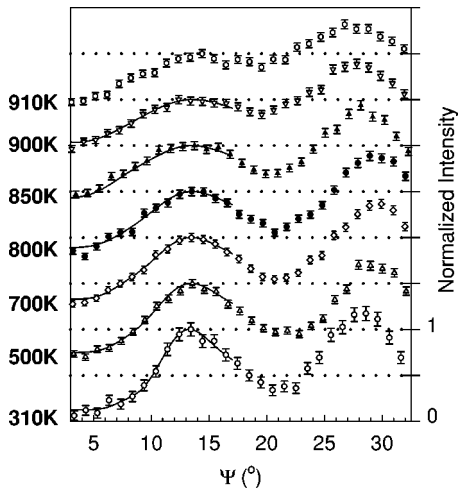

FIG. 7. Symbols are NICISS scans measured along the $\langle 001 \rangle$ azimuthal direction at increasing surface temperature reported on the left *y* axis. The spectra are normalized to the first peak maximum after subtraction of the constant background at room temperature. Solid lines are the best-fitting total scattered intensities.

direction the focusing peak remains detectable well above the critical temperature and flattens first above 900 K. Taking in mind this result we conclude that correlation between the first-neighbor position is retained within the quasiliquid layer also along the $\langle 001 \rangle$ azimuth. To obtain a quantitative estimation of the first focusing peak broadening the two-atom scattering model previously described is adopted to fit the data and the best-fitting curves are superimposed on the spectra in Fig. 7. It can be noted that the quality of the fit is reasonable up to ~ 900 K although the agreement with calculations gets worse with increasing temperature. This can probably be ascribed to the oversimplification within the two-atom scattering model as pointed out in Ref. 21 for Ne^+, 2-keV ion scattering in the NICISS mode on Ag(110). From the present results a suggestion is obtained for a strong increase of the vacancy percentage with temperature in good agreement with the result of Fig. 4. However, since vacancy scattering contributions correspond to incidence angles $\psi \leqslant 8°$ (see, for instance, Fig. 3), they partly merge into the background and the corresponding estimation becomes inaccurate, especially at high temperatures. The perpendicular mean-square vibration amplitude $\langle u_z^2 \rangle$ obtained as fitting parameter is reported versus temperature in Fig. 8. The data follow a linear behavior up to ~ 700 K as predicted by the Debye model. The Debye temperature estimated in the range 300–700 K is $\Theta_d = (410 \pm 15)$ K. Note that the NICISS measurements along the $\langle 1\bar{1}0 \rangle$ azimuth confirm the predicted trend. Above 800 K strong deviations from the harmonic behavior are finally observed.

IV. DISCUSSION AND CONCLUSION

The measurements reported in the previous section first of all confirm the primary role of point defects and steps in the premelting of Al(110) already pointed out by LEED (Refs. 1 and 3) and x-ray scattering (Ref. 4) experiments. The defect

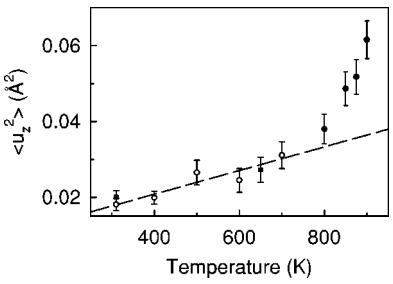

FIG. 8. Evolution of the mean square vibration amplitude $\langle u_z^2 \rangle$ with temperature. Circles and squares refer to NICISS measurements along the $\langle 001 \rangle$ and $\langle 1\bar{1}0 \rangle$ azimuthal directions, respectively. The dashed line is the linear regression for the open circles.

percentage at different temperatures is estimated using LEIS in backscattering mode. This configuration is especially suited to detect surface defects since the probe-defect interaction time for a He^+ beam at 1.5 keV is in the range of a few fs, hence very short with respect to the defect lifetime. In detail, the present estimation of about 10% of surface vacancies at room temperature seems quite large with respect to the predictions of MD simulations[6,7,12] but a similar result is obtained with LEIS well below the surface melting point on Pb(110).[13,14] Moreover, the observed increase of the vacancy percentage up to 24% at 650 K supports well the microscopic description of thermal disordering provided by MD which suggests adatom-vacancy proliferation above 600 K as precursor to surface melting. Analyzing the temperature dependence of the mean-square vibration amplitude of the top-layer atoms strong anharmonic contributions are observed with x-ray scattering above 700 K in agreement with the present result.[4] Comparing the present estimations with those we found in the literature excellent agreement is obtained with the results of MEIS,[22] LEED,[2] and MD simulations[7] while, in Ref. 12, $\langle u_z^2 \rangle$ seems slightly overestimated by MD. Finally, the premelting transition is investigated in the present study along the two main $\langle 001 \rangle$ and $\langle 1\bar{1}0 \rangle$ azimuthal directions. In particular, a new method is adopted along the $\langle 1\bar{1}0 \rangle$ azimuth where the evolution of the channeling peak shape with temperature is followed. Note that the channeling peak arises from ions steered between surface atom rows; hence, it provides information on the crystal order within the outmost layer over a range comparable with typical ion trajectory lengths.[23] Simulations performed for a He^+ ion beam at ~ 2 keV on a defect-free Ni(110) surface show typical channeling lengths of ~ 48 Å along the $\langle 1\bar{1}0 \rangle$ azimuth corresponding to ~ 20 Ni row atoms and to a probe-substrate interaction time in the range of ~ 20 fs.[24] Although detailed simulations must be carried out to get a quantitative picture from the data of Fig. 6, some qualitative results are pointed out. First, it can be noted that the shape of the peak is almost unchanged up to the onset of the premelting transition at 800 K, hence confirming that crystal order is well retained in the considered temperature range along the $\langle 1\bar{1}0 \rangle$ chains. Surface roughness causes a small increase of the peak tail intensity around 600 K which is observed to disappear on approaching premelting, i.e., at 700 K. Note that LEIS in the

channeling mode seems to be poorly sensible to surface vacancies probably because of long channeling trajectories which are almost unperturbed by point defects within the atom rows. Above 800 K the channeling peak starts to merge into the background but a broad maximum is detected even at 890 K, showing that residual crystal order is retained within the surface quasiliquid layer. Quite surprisingly, a similar result is obtained along the perpendicular $\langle 001 \rangle$ azimuthal direction where the evolution with temperature of the NICISS first-focusing peak profile is studied. Here, the peak is observed to strongly broaden above 800 K and to disappear first above 900 K. With respect to the model suggested by Polčic *et al.*[10,11] we remark that good agreement is obtained with the SEXAFS results taking into account that they are limited to the $\langle 1\bar{1}0 \rangle$ azimuth. Therefore, to explain the present data we extend the previous model suggesting that the quasiliquid layer is not constituted by $\langle 1\bar{1}0 \rangle$ atomic chains but rather by two-dimensional clusters of surface atoms in collective motion against each other. This picture is well supported by the results of MEIS and quasielastic He atom scattering studies on Pb(110) showing that residual crystalline order is retained at surface premelting.[25,26] Finally, it is worth noting that similar results are obtained by MD simulations on a very different system, i.e., ~100-atom argon clusters where surface premelting is not associated with amorphous, random surface structures in irregular motion, but rather with organized, collective motion of most of the surface atoms accompanied by a few detached atoms and holes.[27]

In conclusion, LEIS is used in this paper to investigate the evolution of thermal disorder on the (110) surface of aluminum along the $\langle 1\bar{1}0 \rangle$ and $\langle 001 \rangle$ azimuthal directions. Point defects and surface roughness are proven to strongly increase above 600 K. With further increasing temperature surface premelting is observed, studying the evolution of the channeling peak shape. This is, at least to our knowledge, a new technique. Experimental evidence for residual short-range order is obtained along both azimuths within the quasiliquid layer and the suggestion is given that it probably consists of groups of surface atoms performing correlated motions.

ACKNOWLEDGMENTS

We are indebted to Professor R. Tatarek for carefully reading the manuscript. This work was supported by the Deutsche Forschungsgemeinschaft (DFG) and by the Italian MURST through Grant No. 9902112831. Financial support by the Deutsche Akademische Austauschdienst (DAAD) and by the Conferenza dei Rettori delle Università Italiane (CRUI) is also gratefully acknowledged.

*Electronic address: pedemont@fisica.unige.it

[1] A. Pavlovska, M. Tikhov, Yingjun Gu, and E. Bauer, Surf. Sci. **278**, 303 (1992).
[2] H. Göbel and P. von Blanckenhagen, Phys. Rev. B **47**, 2378 (1993).
[3] M. Schwarz, C. Mayer, P. von Blanckenhagen, and W. Schommers, Surf. Rev. Lett. **4**, 1095 (1997).
[4] H. Dosch, T. Höfer, J. Peisl, and L. Johnson, Europhys. Lett. **15**, 527 (1991).
[5] P. von Blanckenhagen, W. Schommers, and V. Voegele, J. Vac. Sci. Technol. A **5**, 649 (1987).
[6] P. Stoltze, J. Chem. Phys. **92**, 6306 (1990).
[7] N. Marzari, D. Vanderblit, A. De Vita, and M. Payne, Phys. Rev. Lett. **82**, 3296 (1999).
[8] A. D. van der Gon, R. Smith, J. Gay, and D. O'Connor, Surf. Sci. **227**, 143 (1990).
[9] W. Theis and K. Horn, Phys. Rev. B **51**, 7157 (1995).
[10] M. Polčic, L. Wilde, and J. Haase, Phys. Rev. Lett. **78**, 491 (1997).
[11] M. Polčic, L. Wilde, and J. Haase, Surf. Sci. **405**, 112 (1998).
[12] D. Shu, D. Sun, X. Gong, and W. Lau, Surf. Sci. **441**, 206 (1999).
[13] S. Speller, M. Schleberger, A. Niehof, and W. Heiland, Phys. Rev. Lett. **68**, 3452 (1992).
[14] S. Speller, M. Schleberger, and W. Heiland, Surf. Sci. **269/270**, 229 (1992).
[15] J. Möller, W. Heiland, K. Snowdon, and H. Niehus, Surf. Sci. **178**, 475 (1986).
[16] A. Niehof and W. Heiland, Nucl. Instrum. Methods Phys. Res. B **48**, 306 (1990).
[17] H. Niehus, W. Heiland, and E. Taglauer, Surf. Sci. Rep. **17**, 213 (1993).
[18] W. Heiland, Vacuum **39**, 367 (1989).
[19] J. Möller, H. Niehus, and W. Heiland, Surf. Sci. **166**, L111 (1986).
[20] L. Pedemonte, R. Tatarek, M. Aschoff, K. Brüning, and W. Heiland, Nucl. Instrum. Methods Phys. Res. B **164/165**, 645 (2000).
[21] L. Pedemonte, G. Bracco, R. Tatarek, R. Beikler, E. Taglauer, K. Brüning, and W. Heiland, Nucl. Instrum. Methods Phys. Res. B **193**, 562 (2002).
[22] B. Busch and T. Gustafsson, Phys. Rev. B **61**, 16 097 (2000).
[23] S. Speller, M. Schleberger, and W. Heiland, Surf. Sci. **380**, 1 (1997).
[24] A. Närmann, W. Heiland, R. Monreal, F. Flores, and P. Echenique, Phys. Rev. B **44**, 2003 (1991).
[25] A. D. van der Gon, H. van Pinxteren, J. Frenken, and J. van der Veen, Surf. Sci. **244**, 259 (1991).
[26] J. Frenken, B. Hinch, J. Toennies, and C. Wöll, Phys. Rev. B **41**, 938 (1990).
[27] H. Cheng and R. Berry, Phys. Rev. A **45**, 7969 (1992).